How fast do structures emerge in hypercycle-systems?

Stephan Altmeyer, Claus Wilke, and Thomas Martinetz
Institut für Neuroinformatik
Ruhr-Universität Bochum
D-44780 Bochum, Germany
Stephan.Altmeyer@neuroinformatik.ruhr-uni-bochum.de

September 18, 2001

Abstract

A general framework for the simulation of reaction-diffusion systems with probabilistic cellular automata is presented. The basic reaction probabilities of the chemical model translate directly into the transition rules of the automaton, thus allowing a clear comparison between simulation results and analytic calculations. This framework is then applied to simulations of hypercycle-systems in up to three dimensions.
Furthermore, a new measurement quantity is introduced and applied to the hypercycle-systems in two and three dimensions. It can be shown that this quantity can be interpreted as a measure for the macroscopic order of the hypercycle systems.

1 The automaton

In the past a lot of work was done in the field of algorithmic chemistry [1, 2] and chemistry on cellular automata (CA) [3, 4]. Our goal is to give a complete framework which begins with the determination of the transition rules from basic reaction probabilities and ends with the comparison between the emergence of spatially ordered structures and a macroscopic measurement quantity in hypercycle-systems.
In this paper we can only give a brief introduction of our probabilistic CA with asynchronous updating. Our aim was to establish a one-to-one correspondence between real chemical reactions (defined by their reaction probabilities) and the simulations on a CA (defined by the transition rules). Therefore, we explain the calculation of these transition rules for a simple particle production process in detail and then present the transition rules for more complex reaction types without derivation.

1.1 Particle production processes

In our system, particles can be produced through spontaneous or induced reactions. The result of both reactions is the change of an empty cell to an occupied one. Since we evaluate production processes for empty cells, we will usually have the situation that several different reactions are possible, resulting in a different final state for the previously empty cell. If we think, e.g. of spontaneous self-replication, all the nearest neighbors of the empty cell are in principle equally likely to reproduce into this cell. In chemistry such symmetry breaking phenomena are induced by statistical fluctuations, e.g. temperature gradients.

Let $p_i,\ i \in \mathcal{A}$, be the probability for a single species i to replicate into the empty cell by a special reaction, e.g. self-replication. Here $\mathcal{A}$ denotes an index set containing all indices which are necessary to enumerate all species in the given context and N_i will denote the number of molecules of species i.

In the case there are several nearest neighbor cells occupied, we first have to calculate the total probability p^{tot} that at least one arbitrary nearest-neighbor-molecule will occupy the empty cell. We get

$$p^{\text{tot}} = 1 - \prod_{i \in \mathcal{A}} (1 - p_i)^{N_i}. \tag{1}$$

From p^{tot} we can calculate the effective probabilities for the nearest neighbor molecules to replicate in the given arrangement of species. We will denote these probabilities with p_i^{eff}. In this calculation we have to make sure that the ratio p_i/p_j is equal to $p_i^{\text{eff}}/p_j^{\text{eff}}$, $\forall i, j \in \mathcal{A}$. Since the sum over all p_i is not necessarily 1, we introduce a normalization factor $\sum_{i \in \mathcal{A}} N_i p_i$.[1] We get

$$p_i^{\text{eff}} = p_i \frac{p^{\text{tot}}}{\sum_{i \in \mathcal{A}} N_i p_i}. \tag{2}$$

Note that p^{tot} is the sum of $N_i p_i^{\text{eff}}$ over all i.

1.1.1 Type I reactions

Reactions of type I,

$$M_i \xrightarrow{p_{i,m,n}} M_m + M_n,$$

represent the group of spontaneous reactions with two reaction products. After some work and with the calculations done above we get:

$$p_{i,m,n}^{\text{eff}} = p_{i,m,n} \frac{1 - \prod_{i \in \mathcal{A}} (1 - p_{i,m,n})^{N_i}}{\sum_{i \in \mathcal{A}} N_i p_{i,m,n}}. \tag{3}$$

[1] The normalization factor is introduced to ensure that the sum over all p_i^{eff} and $1 - p^{\text{tot}}$ is 1.

The corresponding transition rule then reads:
A cell with state zero will change to state n and a nearest-neighbor cell with state i will change to m with the probability $p^{\text{eff}}_{i,m,n}$.

1.1.2 Type II reactions

Reactions of type II,

$$M_i + M_j \xrightarrow{p_{i,j,m,n,o}} M_m + M_n + M_o,$$

describe a group of two-body reactions with three reaction products. Obviously, such reaction processes are more difficult to handle since we have to implement the determination of the correct reaction partner. The related quantities are primed.
After some calculations we get:

$$p^{\text{eff}}_{i,j,m,n,o} = p'_{i,j,m,n,o} \frac{1 - \prod_{i\in\mathcal{A}} (1 - p'_{i,j,m,n,o})^{N'_i}}{\sum_{i\in\mathcal{A}} N_i p'_{i,j,m,n,o}}. \tag{4}$$

with

$$p'_{i,j,m,n,o} = p(N' \neq 0) \frac{N'_j}{N'} p_{i,j,m,n,o}. \tag{5}$$

$p(N' \neq 0)$ denotes the probability that there is at least one molecule to react with. For the derivation of $p'_{i,j,m,n,o}$ we have implicitly used the idea of an attractive force between the molecules which means that the reactive molecule therefore "jumps" to a reaction partner. On the other hand, if we do not assume such an attractive force, which means a molecule can also "jump" into a hole, we have to substitute $p'_{i,j,m,n,o}$ with $N'_j/N'_{\max}$.
Then we can write down the transition rule:
The probability that a cell in state zero, with a nearest-neighbor cell in state i and with a "reaction" cell in state j will change to o, while the nearest-neighbor cell changes to m and the "reaction" cell changes to n, is $p^{\text{eff}}_{i,j,m,n,o}$.

1.1.3 Particle decay

The decay process,

$$M_i \xrightarrow{p^{\text{dec}}_i} 0,$$

can change an occupied cell into an empty one. The transition rule description is rather easy:
The probability that a cell in state i will change to a cell in state zero is p^{dec}_i.

1.2 Diffusion

The diffusion is an additional process. Since we use an asynchronous automaton, an often used diffusion algorithm for CA [5] is not necessary. Instead, we use a more natural algorithm that can be divided into three subprocesses:

1. An arbitrary cell of the CA is chosen.
2. One of it's nearest neighbor cells is determined at random.
3. The states of the two cells are interchanged.

1.3 Automaton update

We use asynchronous updating, since this seems to be the more natural way [6]. The basic processes are then executed in the following way:
Choose an arbitrary cell at random. If the cell is occupied we use the decay-transition rule. Otherwise the transition rule for reactions of type I or of type II or a combination of both are used.
The reaction processes and the diffusion process are then combined to the full simulation in the following way. Let k be the total number of cells in a CA and d the ratio of the number of basic processes and the number of diffusion steps. Then a CA-time-step t consists of k basic processes and dk diffusion steps. It is important that the basic processes and the diffusion steps are mixed up very well.
Note that t is independent of the system's size, since we scale the number internal processes with it.

2 Simulation

We have simulated systems with (symmetrical) hypercycles [7, 8], which means we set

$$p_{i,j,k} = \begin{cases} p^{\text{self}} & \text{if } i = j = k, \\ 0 & \text{else} \end{cases} \tag{6}$$

and

$$p_{i,j,m,n,o} = \begin{cases} p^{\text{cat}} & \text{if } i = m = o, j = n \text{ and } i = j + 1 \text{ (cyclic)}, \\ 0 & \text{else} \end{cases} \tag{7}$$

2.1 Stable patterns

In this part of the paper we will show the well-known spiral waves [4] in two dimensions and the emergence of a stable scroll wave structures [9] in three dimensions. In the latter case we have used a two-dimensional spiral as initial condition. We will see the system going through different unstable patterns. For reasons of clear visualization, in the pictures we show only one of the six species present in the simulation.
The three-dimensional analog of a spiral wave is a scroll wave [9]. As we can see in Fig. 3, even in the two dimensional case, structures can be very complex. Since there are more degrees of freedom in three spatial dimensions, the structures arising from non-ordered initial conditions are much more complex. Therefore, we use a 2d spiral as a symmetry-breaking initial condition for our simulations to simplify the emergent structures.
We can see the spiral's growth in the z-direction (see Fig. 1, 2). As a matter of fact, the reproduction activity of a species becomes high if it is adjacent to it's "supporter". Therefore, in a layer above, molecules are first created over the small region where their own and their "supporter" are present. Since the spirals rotate in the "supporter" direction, we can see the phenomenon that the new spirals, growing on top of the old ones, are phase shifted in the rotation direction. This continues until the space in z-direction is occupied. The resulting structure looks like a rotating screw. When all the available space is occupied, the molecules cannot replicate freely any more. Since space is rare than, the molecules have to compete for empty space to replicate. For this reason, the molecules begin to arrange themselves in a different way so that the "free" screw begins to change to a cone structure. This cone structure is stable so that a real scroll wave cannot be seen.
The whole re-arrangement process takes much more time than the occupation at the beginning. The pictures show the emergence of the cone structure. At the top of the cone the emergence of other small cones can be seen so that the whole structure becomes more complex.

2.2 A microscopic measurement quantity

Now we will introduce a measurement quantity with which we can measure the arrangement of the molecules in our automaton. The definition of this order-quantity, called α_k, is rather easy:
For every molecule, we take the nearest neighbor molecules. If an adjacent molecule is a "supporter", the variable S is incremented by one. Otherwise the variable N is incremented by one. If a cell is not occupied, nothing is done. With these microscopic values we can define the macroscopic quantity

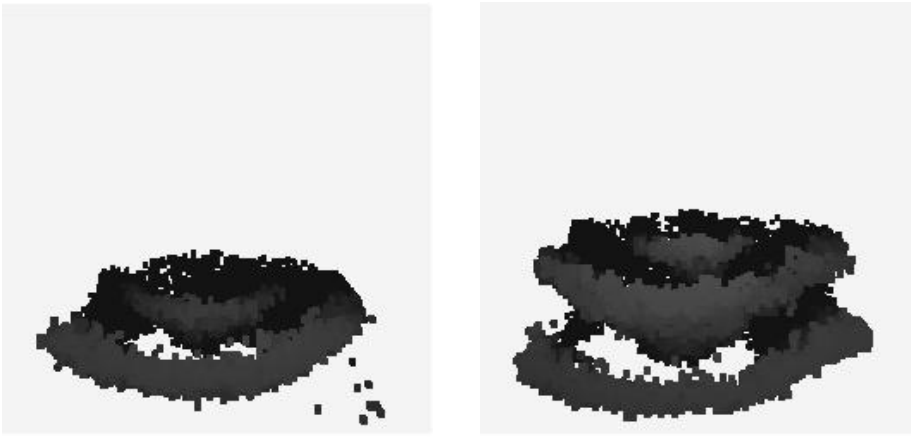

Figure 1: The first two pictures show the system's behavior shortly after the "injection" of the 2d spiral. We can see the emergence of a rotating screw. The left picture was taken at $t = 150$ and the right one at $t = 250$.

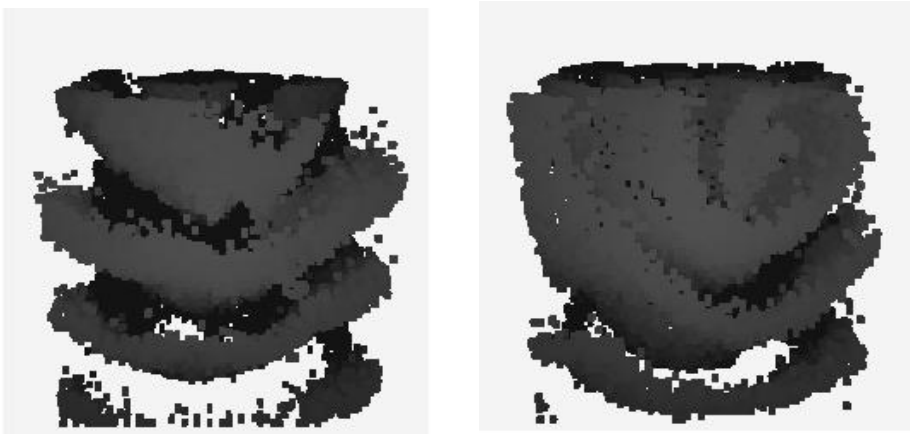

Figure 2: If the space is nearly completely occupied the molecules cannot replicate freely and have to compete for empty space. Therefore the structure changes from a screw to a cone-like pattern.

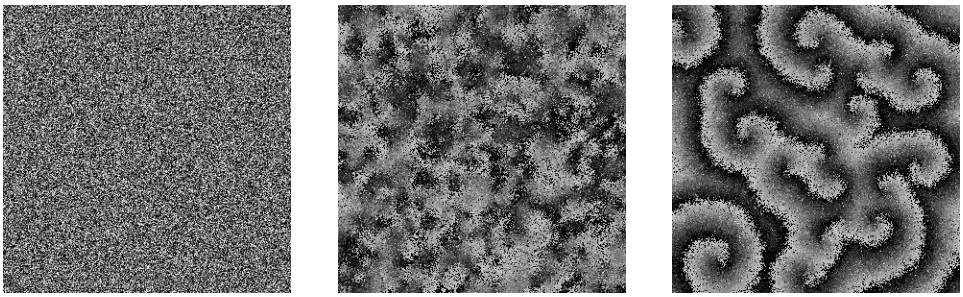

Figure 3: The three pictures show the time dependent behavior of the system. The times when the pictures have been taken are (from left to right): $t = 0$, $t = 120$ and $t = 9000$. See also Fig. 4 and text for further information.

α_k:

$$\alpha_k = \frac{kS}{N + kS}, \tag{8}$$

where $k \geq 0$ is a tuning constant. The larger k, the more sensitive is α_k on S.
Since both $N, S \geq 0$, the quantity α_k ranges between 0 and 1. We will later see that α_k is even constant for large t. (Obviously, if α_k is constant, $\alpha_{k'}$, with another $k' \neq k$, is also constant.)
Moreover, since we do not take into account empty cells, α_k is independent of the system's concentration and therefore independent of p^{dec}.
For our simulations we have used $k = 10$ and applied α_{10} to both the two and three dimensional case.
Note that there are a lot of possible microscopic/macroscopic quantities which all can describe the system from different points of view.

2.3 Two dimensions

For the two dimensional case we have used two different initial conditions. In both cases the parameter set is $p^{\text{dec}} = 0.1$, $p^{\text{self}} = 0.05$, $p^{\text{cat}} = 0.9$ and $d = 1$.

First, the hypercycle-system was initialized at random, see Fig. 3. We have seen α_{10} converging rapidly to a constant value at the very beginning. After $t = 120$, however, α_{10} changes only in very small amounts. In comparison, the global structure of the system also changes very slowly, see Fig. 4. It seems that the system's rough structure is determined at the very beginning and will then only be refined, later on. This is very interesting, since there are a lot of possible stable patterns. However, the decision is made very early.
For the asymptotic value of α_{10} we have found $\alpha_{10} \approx 0.72$, independent

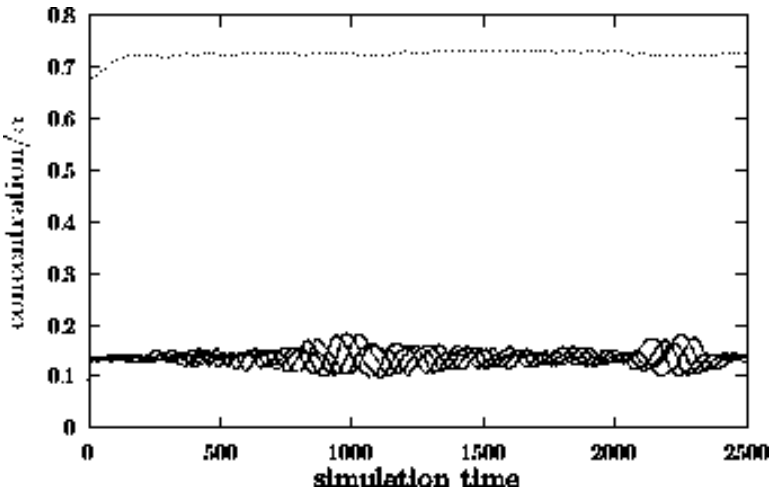

Figure 4: The picture shows the concentrations of the six hypercycle species (solid lines) and the value of α_{10} versus time for a system with random initial condition.

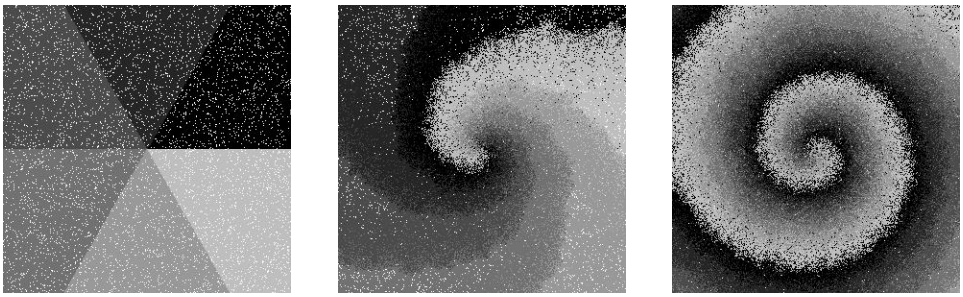

Figure 5: The three pictures show the time dependent behavior of the system. The times when the pictures have been taken are (from left to right): $t = 0$, $t = 140$ and $t = 550$. See also Fig. 6 and text for further information.

of the number of species in the hypercycle and of the system's size. Furthermore, α_k depends only weakly on d for $d < 1$. The next step was to examine a system where only one stable final pattern exits. Therefore, we have used a special initial condition which is displayed in Fig. 5. The final structure will be of course a single rotating spiral.
What we have seen was α_{10} changing comparably to the transformation of the triangular structure to the spiral structure. Since the major part of this transformation is done at the beginning, α also increases fast during the first simulation steps and then increases slower and slower. The system behaves similar to the case with random initialization, although the convergence of α_k to it's asymptotic value is significantly slower. But what is more surprising, the asymptotic value of α_{10} is again the same, $\alpha_{10} \approx 0.72$.

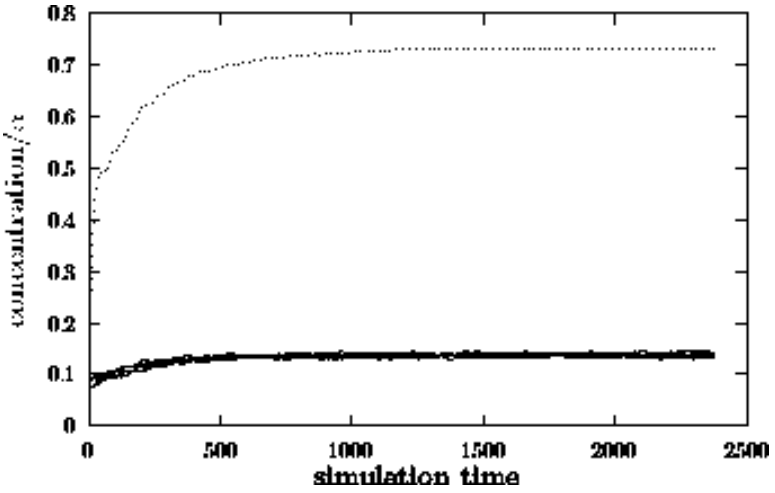

Figure 6: The picture shows the concentrations of the six hypercycle species (solid lines) and the value of α_{10} versus time for a system with ordered triangles as initial condition.

We will now go a step beyond and apply α_{10} on our three dimensional simulator.

2.4 Three dimensions

As we have seen above (Fig. 1, 2) in three dimensions there are several different unstable structures, beginning with a single two dimensional spiral as initial condition and ending with a stable cone-structure.
In Fig. 7 we can see α_{10} starting with $\alpha_{10} \approx 0.72$. But then we see α_k increasing in the time interval when the spiral occupies the empty space by growing in the z-direction. After that, when the available space is occupied, new boundaries are present and α_{10} decreases to the former value.
This is a bit surprising since the cone structures are quite different and at the first glance there seems to be no reason why the macroscopic order should be similar.

3 Conclusions

In this paper we have shown pictures of the transformation from two dimensional patterns to three dimensional ones and have therefore seen the system walking through different states of arrangement. But what is more interesting is the fact that our macroscopic quantity α_k (here: α_{10}) is quite constant after a short time and has even the same asymptotic value in different settings.
In all our simulations, especially in two dimensions, we have seen α_{10} con-

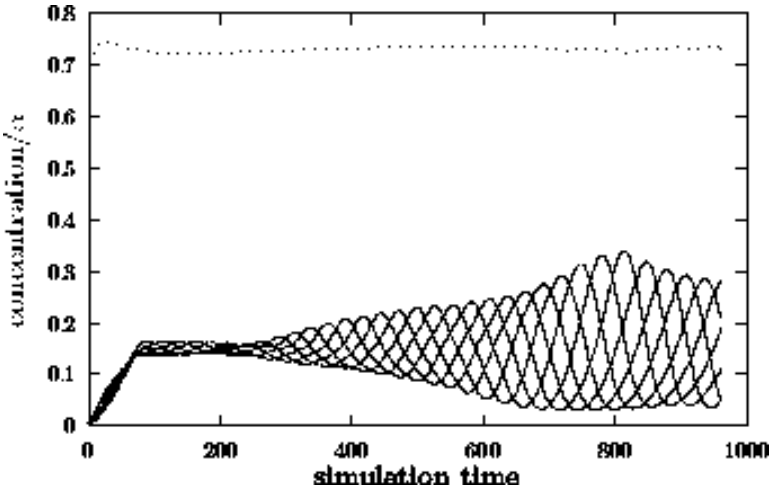

Figure 7: The picture shows the concentrations of the six hypercycle species (solid lines) and the value of α_{10} versus time for a system in three spatial dimensions. Note that a single two dimensional spiral was used as initial condition.

verging rapidly to the fixed value, $\alpha_{10} \approx 0.72$. Thereof we can deduce that such catalytic systems have the urge to determine their final structures at the very beginning. Later on structures are only refined.
Although the hypercycles have been studied very well in the past years some new features can still be found. We think that the definition of microscopic quantities and their interpretation in a macroscopic sense is one of the right ways to learn more about catalytic systems which can be even more complex than such "simple" symmetric hypercycles.

4 Outlook

It seems to be interesting for future work to study whether stability against parasites is possible in three dimensions, similar to the two-dimensional case [4, 10]. Furthermore, the behavior of α_k in such parasite-systems might be interesting.

References

[1] R. J. Bagley and J. D. Farmer. Spontaneous emergence of a metabolism. In C. Langton, C. Taylor, J. Farmer, and S. Rasmussen, editors, *Artificial Life II*. Santa Fe Institut, Addison-Wesley, 1992.

[2] R. J. Bagley, J. D. Farmer, and W. Fontana. Evolution of a metabolism. In C. Langton, C. Taylor, J. Farmer, and S. Rasmussen, editors, *Artificial Life II*. Santa Fe Institut, Addison-Wesley, 1992.

[3] M. Gerhardt, H. Schuster, and J. J. Tyson. A cellular automaton describing the formation of spatially ordered structures in chemical systems. *Physica D*, 36, 1989.

[4] M. Boerlijst and P. Hogeweg. Self-structuring and selection: Spiral waves as a substrate for prebiotic evolution. In C. Langton, C. Taylor, J. Farmer, and S. Rasmussen, editors, *Artificial Life II*. Santa Fe Institut, Addison-Wesley, 1992.

[5] T. Toffoli and N. Margolus. *Cellular Automata Machines*. MIT Press, 1987.

[6] I. Harvey and T. Bossomaier. Time out of joint: Attractors in random boolean networks. In P. Husbands and I. Harvey, editors, *Fourth European Conference on Artificial Life*. MIT Press, 1997.

[7] M. Eigen and P. Schuster. *The Hypercycle: A Principle of Natural Self-Organisation*. Springer, 1979.

[8] J. Hofbauer and K. Sigmund. *The Theory of Evolution and Dynamical Systems*. Cambridge University Press, 1988.

[9] J. J. Tyson and J. P. Keener. Singular pertubation theory of travelling waves in excitable media. *Physica D*, 32:327–361, 1988.

[10] M. Cronhjort and C. Blomberg. Chasing: A mechanism for resistance against parasites in self-replicating systems. In C. Langton and K. Shimohara, editors, *Artificial Life V*. MIT Press, 1996.